Processing TIRF Microscopy Images to Characterize the Dynamics and Morphology of Bacterial Actin-Like Assemblies

Cyrille Billaudeau, Arnaud Chastanet, Rut Carballido-Lopez

Chapter 9

Processing TIRF Microscopy Images to Characterize the Dynamics and Morphology of Bacterial Actin-Like Assemblies

Cyrille Billaudeau, Arnaud Chastanet, and Rut Carballido-López

Abstract

Total internal reflection fluorescence (TIRF) microscopy allows the visualization of the dynamic membrane-associated actin-like MreB filaments in live bacterial cells with high temporal resolution. This chapter describes computerized analysis methods to quantitatively characterize the dynamics and morphological properties of MreB assemblies. These include how to (1) segment bacterial cells, (2) perform single-particle tracking (SPT) of MreB filamentous structures, (3) classify their dynamic modes using mean squared displacement (MSD) analysis, and (4) measure their dimensions and orientation.

Key words Image analysis, MreB, Single-particle tracking (SPT), Automated dynamic classification, Mean squared displacement (MSD), Kymograph, 2D anisotropic Gaussian fitting

1 Introduction

MreB proteins are actin homologs essential for rod-shaped determination in bacteria [1, 2]. They polymerize into membrane-associated short filaments that are distributed along the sidewalls and exhibit several dynamic behaviors including processive circumferential motion around the short axis of the cell, random diffusion, and constrained diffusion [3–5]. Characterization of the localization and dynamics of MreB assemblies in the membrane requires fluorescence microscopy techniques providing high optical sectioning, high spatial resolution, fast acquisitions, and low photobleaching during acquisitions. Total internal reflection fluorescence microscopy (TIRFM), an elegant optical technique that selectively excites fluorophores in a thin region (<200 nm) at the coverslip/sample interface [6, 7], successfully allows quantitative analysis of MreB in live cells [3–5] (*see* Chapter 8 and **Note 1**).

The first quantifications of the velocity of MreB assemblies exhibiting directed motion around the cell periphery were
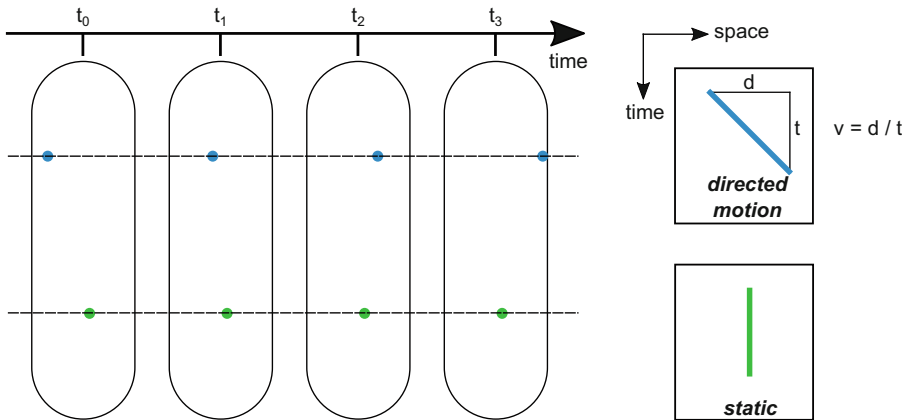
Fig. 1 Principle of kymograph analysis. Kymograph analysis allows to represent a dynamic process in a single image (kymogram). A line (dotted lines) is drawn on a time-lapse sequence of images, and the intensities are reported in a time-space plot. The resulting kymograms depend on the particle dynamics: tilted lines for directed motions (blue) or vertical lines (parallel to the time axis) for static objects (green). Speed (*v*) of directed particles is calculated from the line slope of the distance (*d*) over time (*t*)

performed using kymograph analysis [4, 5], a simple but efficient method to represent the dynamics of moving structures on a two-dimensional image (a kymogram). Kymograms allow a direct readout of speed, direction, and intensity of motile structures. Kymograph analysis of time-lapse TIRFM acquisitions is generated by drawing a line over a trajectory and plotting the intensity along this line for all the time frames of the stack. A dedicated software provides a space-time (*x-t*) plot where the vertical axis represents time and the horizontal axis corresponds to the intensity of the pixels along the length of the selected trajectory. Depending on the dynamic nature of the object, kymograms display vertical lines parallel to the time axis (static objects) or tilted lines (moving objects) (Fig. 1). The slope of moving objects gives a measurement of the velocity and direction of motion of the object (Fig. 1).

Although kymograph analysis is easy to implement, it only allows studying directed motions or static behaviors, whereas motility can be more diverse and include diffusive and mixed behaviors. Single-particle tracking (SPT) combined with mean squared displacement (MSD) analysis is an alternative approach that provides quantitative information of the dynamic behavior of individual objects and can help to determine whether a particle is freely diffusing, confined, or actively transported. In SPT, tracks (or particle trajectories) are obtained by detecting the individual particles in the acquired image sequences and by reconnecting them between consecutive time frames. Many open-source (e.g., u-track [8], TrackMate [9]) and customized tracking algorithms have been developed using different strategies to efficiently detect particles and take into account their dynamic properties. The mode
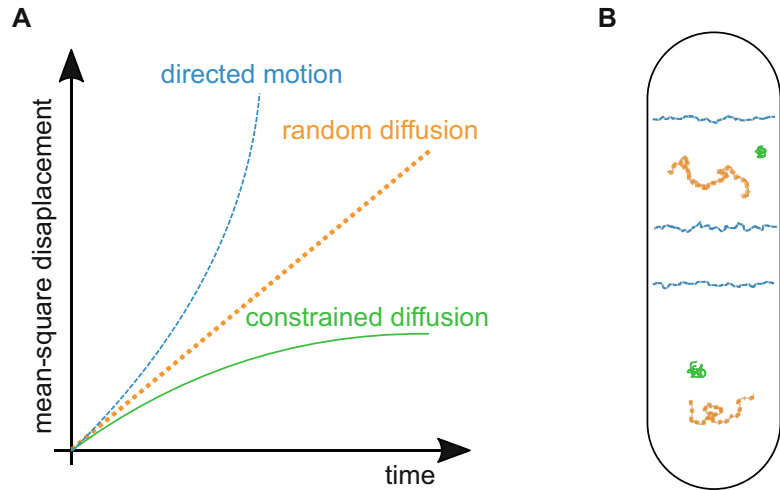
Fig. 2 Principle of mean square displacement analysis. (**A**) MSD curves allow the classification of the mode of movement: (1) Second-order polynomial fit indicates directed motion (blue): $MSD(t) = (\nu t)^2$, where ν is speed and t is time; (2) a linear plot indicates random diffusion (orange): $MSD(t) = 4Dt$, where D is the diffusion constant; (3) when the MSD curve reaches a plateau, the system is undergoing constrained diffusion (green). (**B**) Representation of 2D-SPT trajectories (following the above-mentioned color code) of the three modes of MreB motion in the membrane of a rod-shaped cell

of displacement is determined from the resulting trajectories by calculating the so-called mean squared displacement. The MSD describes the average of the squared distances between the starting position of a particle and its end position over time for all time lags of certain length Δt within one trajectory. The properties of the resulting MSD versus t plots are indicative of the dynamic regime of the particle: linear MSD for random diffusion, quadratic for transported/directional movement, and asymptotic for bound/trapped/constrained motion, not freely diffusing (Fig. 2). The type of motion of a given particle is then automatically classified by a curve fitting.

In this chapter, we first describe how to segment cells automatically for the analysis of MreB assemblies. Next, we detail how to apply kymograph and MSD analysis to determine their dynamic behavior and to quantify their main features (velocity, direction, diffusion coefficient). Finally, we present two different approaches to measure the dimensions of MreB filamentous structures. The first method relies on 2D spatial fitting to extract the length and the width of objects of dimensions close to the spatial resolution. The second strategy is based on kymograph analysis and more adapted to determine the length of longer objects.

2   Materials

1. Time-lapse TIRFM acquisitions of MreB (or of your membrane protein or membrane-associated protein of interest) labeled with a fluorescent probe (i.e., fused to a fluorescent protein such as GFP or to an affinity tag binding a fluorescent ligand such as SNAP tag or Halo tag) in live bacterial cells (*see* Chapter 8). Frame rate, exposure time, and total duration of the time lapse should be adapted to the dynamics of the protein and to reduce photobleaching as much as possible during the image sequence acquisition (*see* **Note 2**). The sequence of images (stack) should be saved in TIFF format in 16-bit gray scale. Be sure that all acquisition settings, such as pixel size and time interval between consecutive frames in a movie, are accessible from the image metadata (*see* **Note 3**). If needed, correct the drift in the image sequence (*see* **Note 4**).

2. A computer with an installation of the Fiji open-source software (http://fiji.sc/#download [10]) and of Matlab (*see* **Note 5**).

3. Homemade script macros available on GitHub website: SegCells_TIRF.ijm and KymographAnalyzer.ijm (Fiji); patchDynamicClassification_MSD.m (Matlab).

4. u-track software (version 2.1.3, Matlab-based suite) [8, 11]: u-track offers different detection and reconnection approaches depending on the object shape (isotropic vs. anisotropic) and density (single vs. multiple 2D Gaussian fitting) and its dynamic properties (free diffusion, directed, disappearance, merge/spilt events, etc.).

3   Methods

3.1   Automated Cell Segmentation of TIRF Sections

Cell segmentation is an essential step in quantitative subcellular analysis. Many automated cell segmentation algorithms have been developed to determine the cell outline from phase contrast images or from membrane-stained cells (e.g., MicrobJ [12], Oufti [13], SuperSegger [14]). In TIRF microscopy, only the cell section located in the vicinity (~100–200 nm depth) of the coverslip is excited by the evanescent field (*see* Chapter 8). Because of the dimensions of bacterial cells (e.g., ~3 μm long × 1 μm wide for *Bacillus subtilis* or *Escherichia coli*), this optical section thickness is approximately the uppermost one-fifth of the cell diameter, and thus the TIRF visible cross section is smaller than the cell diameter. Therefore, the density of membrane particles would be systematically underestimated if cells are segmented from phase contrast images due to the estimation error on the cell area. Thus, it is recommended to segment cells directly from TIRF images, as follows:

1. Apply a Gaussian filter to the image, and generate a mask image resulting from the maximal intensity projection (MIP).

2. Identify and label single cells by thresholding the resulting MIP image, and if needed, (a) group over-segmented cells or (b) disconnect neighbored cells included in a single region of interest.

The resulting output should be a mask image where the TIRF sections of single cells visible in a field of view are specifically identified. Pixel values of the mask would be either null for background or a positive integer for the cell. The script macro SegCells_TIRF.ijm segments automatically the cell area under TIRF illumination. To run the macro in Fiji, go to "PluginsMacros/Run…," select the script file, and press the "Run" button in the script window.

3.2 Kymograph-Based Measurement of Particle Velocity

Kymograms can be generated with several tools available in the Fiji software (e.g., Reslice command, Multi Kymograph, Kymograph-Builder), but quantification of particle velocity has to be done manually. We developed for this the dedicated macro KymographAnalyser.ijm, which generates kymograms and automatically determines the speed of particles. Run the macro in Fiji (go to "PluginsMacros/Run…," select the file, and press the "Run" button in script windows). The macro will:

1. Ask the user to draw manually a line on each particle trajectory and add all lines in the ROI manager.

2. Automatically generate the corresponding kymograms (based on the "Reslice" command).

3. Detect automatically the intensity maxima in a user-defined rectangular selection of the kymogram and measure velocity as the line slope using a linear regression (Fig. 1).

Velocity should be measured on many cells from independent experiments in order to provide statistically significant datasets.

3.3 Automatic Classification of Particle Dynamics

1. Once the raw images have been correctly converted to a stack and drift-corrected, and the cells have been segmented, SPT is executed to obtain the trajectories of the objects, which will then be analyzed by MSD.

2. Run u-track on Matlab by typing movieSelectorGUI.m in the command window to launch the graphical user interface (GUI). A first window allows editing and saving the list of image stacks to be analyzed and to specify the acquisition settings (e.g., pixel size, objective numerical aperture, excitation/emission wavelength, exposure time).

Table 1

Main parameters used for single-particle tracking of MreB assemblies using the u-track Matlab-based package

Object detection (Comet detection)	Difference of Gaussian Watershed-based segmentation	$\sigma_1 = 1$ pixels, $\sigma_2 = 4$ pixels Minimum threshold = 4 standard deviation (s.d.) of image intensity, with a step size = 1 s.d.
Object linking	Particles exhibit random motion or directed movement	$0 <$ Brownian search radius < 3 pixels
	No missing link allowed Splitting or merging of tracks not allowed	Maximal gap to close = 0

Pixel size = 64 nm

3. After validating and saving the images list, select "2D single-particle tracking" to configure the two main steps of SPT (all parameters are listed in Table 1). Object detection is performed using the comet detection method, which relies on structure enhancement (by a difference of Gaussian filter), followed by watershed segmentation. Object reconnection allows to link detections from frame to frame, assuming both diffusion and directional movement. The algorithm can also consider some more complex situations during reconnection as gap-closing events (spot disappearance for one frame because it moves out of focus or the detection fails) or splitting/merging events.

4. After automated particle tracking, it is important to carefully inspect the trajectories generated to verify that detections and reconnections are correct, and to modify analysis parameters when required.

5. Next, membrane particle density is estimated as the temporal average of detected objects on each image divided by the surface area under observation (based on the cell segmentation described in Subheading 3.1).

6. Dynamic classification is performed upon MSD analysis using the Matlab script "patchDynamicClassification_MSD.m" (to be typed and executed in the command window of Matlab). To characterize the dynamic properties of MreB assemblies, MSD curves are only computed on tracks of a sufficient minimal duration (i.e., minimal number of steps). Short trajectories are rejected from the analysis so that the main dynamic mode can be identified and the trajectory sampling is adapted to a robust fitting (*see* **Note 6**).

7. The following simple decision tree has been proposed to classify the dynamic mode: constrained, if MSD reaches a plateau below a threshold value to be determined experimentally using

fixed samples (e.g., fluorescent beads) imaged in the same imaging conditions than those used to generate TIRF movies, and mobile, if the maximal MSD value is higher than the threshold value.

8. The mode of movement is then determined based on the analysis of MSD curves using least-square fitting and appropriate models. Second-order polynomial fit ($\mathrm{MSD}(t) = (vt)^2$ where v is speed and t is time) indicates directed motion. A linear plot ($\mathrm{MSD}(t) = (Dt)/4$ (where D is the diffusion constant) indicates random diffusion. Decision between directed motion and free diffusion stands on the comparison of the goodness-of-fit R^2 obtained for each model. The behavior of a particle movement is classified as directed motion if $R^2_{\mathrm{dir}} > 0.8$ and $R^2_{\mathrm{dir}} > R^2_{\mathrm{diff}}$, as random diffusion if $R^2_{\mathrm{diff}} \geq 0.8$ and $R^2_{\mathrm{diff}} > R^2_{\mathrm{dir}}$, and unclassified if $R^2_{\mathrm{dir}} < 0.8$ and $R^2_{\mathrm{diff}} < 0.8$.

9. Upon determination of the type of motion, it is possible to characterize the population by quantifying the corresponding dynamic properties (e.g., velocities, diffusion coefficients, distribution of dynamic modes among the entire population or at the single-cell level).

3.4 Determination of Filament Dimensions and Orientation by 2D Gaussian Fit

This section describes the automatic quantification of the size and orientation of particles observed by TIRFM regardless of their apparent movement (*see* **Note 7**). It is only assumed that MreB assemblies display an anisotropic 2D Gaussian shape without preferential orientation relative to the cell or image axis. Dimensions (length and width) and orientation of filamentous structures (Fig. 3A) can be measured by fitting each particle in the image using the least-square method with a 2D Gaussian function as a model:

$$f(x, y) = B_0 + I_0 \exp\left[-\left(\frac{(x - x_0)\cos(\theta) + (y - y_0)\sin(\theta)}{\sigma_1}\right)^2 - \left(\frac{-(x - x_0)\sin(\theta) + (y - y_0)\cos(\theta)}{\sigma_2}\right)^2\right]$$

where B_0 and I_0 are the background intensity and amplitude of the Gaussian function centered at (x_0, y_0) with lateral widths (σ_1, σ_2) and θ is the orientation of the Gaussian in image coordinates. The length l and width w of filaments are defined as the maximum and minimum values, respectively, of the full width at half-maximum $\left(2\sigma_i\sqrt{(2\log 2)}, i = 1, 2\right)$. To avoid quantification errors, it is recommended to perform the analysis only for isolated filaments and to discard values below the spatial resolution measured experimentally using fluorescent beads. It is important to keep in mind that under TIRF illumination, only ~1/5th of the bacterial cell is
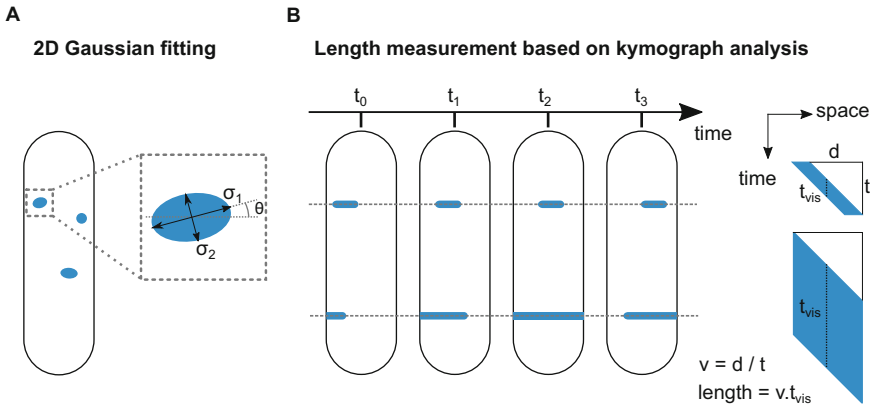
Fig. 3 Determination of the dimensions of filamentous structures. (**A**) Determination of filament dimensions and orientations by 2D Gaussian fit. The dimensions (length, σ_1, and width, σ_2) and orientation (θ) of the filamentous structure are measured by cropping the image area surrounding it and by fitting each object using a least-square method and a 2D anisotropic Gaussian function. (**B**) Quantification of the length of long filaments using kymograph analysis. Profile lines (1 pixel wide, dotted lines) are drawn along separated filament trajectories in order to generate kymographs. While spherical and ellipsoid structures appear as lines (*see* Fig. 1), elongated structures appear as parallelograms. Velocity (v) can be estimated as the angle of the parallelograms. t_{vis} is the time between the appearance of both extremities of a filament at a given position. The length of filaments is estimated as $v \times t_{vis}$

visible (*see* Subheading 3.1 above). Consequently, the length of structures spanning across the TIRF section can be underestimated. To overcome this problem, it is also possible to extract length information using kymographs analysis as described in the next section.

3.5 Determination of the Length of Dynamic Structures Using Kymograph Analysis

The length of structures can also be determined by kymograph analysis (Fig. 3B). This approach is essential for structures longer than the field of view, for which the 2D Gaussian fit method cannot be used. For MreB filaments exhibiting directed motion around the cell circumference, lines (1 pixel wide) are drawn on the trajectories of filaments spatially separated from each other. Intensity maxima are automatically detected along the kymograph and fitted using a linear function to quantify the filament velocity v. The length of each filament is estimated as $v \times t_{vis}$ where t_{vis} is the average time during which the filament is visible on each kymograph position. Only filaments entirely visible (i.e., appearing and disappearing) during the time of acquisition (and excluding the first and last five frames for certainty) are to be used for the analysis.

4   Notes

1. TIRF microscopy allowed single-particle tracking (SPT) of membrane-associated MreB assemblies, revealing their dynamic properties and heterogeneous distribution. TIRFM-

SPT studies based on fluorescent proteins are, however, limited by the density of the imaged proteins in the cell surface. Diffracted emission fluorescence prevents tracking of individual proteins that are separated by less than 0.5 μm. To bypass the limit of resolution of classical light microscopy, it is recommended to perform single-particle tracking with photoactivated localization microscopy (spt-PALM) instead, which is based on temporal emission decorrelation [15].

2. Reliable image quantification requires considering all aspects of the microscopy experiments, from the preparation of the sample to the acquisition settings. Among the parameters to pay particular attention to, exposure time and laser power have to be finely tuned to limit photobleaching but also to use the dynamic range of the camera in full (and avoid the loss of low- and high-signal intensities).

3. Most light microscopes cameras capture 12-bit images, while acquisition softwares mainly propose to save the acquired images in 16-bit or 8-bit formats. Although saving images in the 16-bit file format requires more storage space, it has the advantage of keeping all details of the images. In contrast, saving the acquired images in the 8-bit file format causes the loss of some fine details. This is unsuitable for quantifications requiring sensitivity such as imaging fluorescently labelled proteins in live bacteria (because of the low concentration of molecules in bacterial cells). Note that image files store both the image data (pixel values) and metadata (information on the data that give a sense to the pixel information, such as pixel dimensions, objective lens, excitation light source, emission and acquisition settings, etc.). Some specific file formats like OME-TIFF (hybrid format containing pixel data in TIFF format and metadata in XML format contained in the TIFF header) are well supported in current image processing software (e.g., Fiji using BioFormats) and avoid analysis mistakes by accessing directly to the acquisition settings.

4. During long experiments, temperature changes, dehydration of agarose pads, or mechanical relaxation effects can cause the drift of the sample or of the instrument. In modern microscopes, drift can be limited using an optical table, an environmental temperature-controlled chamber, and/or an automatic focus drift compensation system. Nevertheless, residual drift still occurs in most acquisitions and needs to be corrected. Many algorithms have been developed to correct drift and are readily available and easy to use (e.g., StackReg plugins in ImageJ). It is highly recommended to use one of them for time-lapse observations before processing the image sequence.

5. Requirements for computer: License for Matlab is required, with the Image Processing and Curve Fitting Matlab toolboxes. The software was tested with Matlab versions 2016B and 2018B.

6. A high number of rejected tracks might reflect that the acquisition settings (e.g., laser power, photobleaching, exposure time) and/or the detection and/or linking parameters in SPT have to be corrected. Settings should be optimized to minimize the number of rejected tracks.

7. Lateral resolution in TIRFM is diffraction-limited, and thus dimensions of structures below the limit of resolution (∼250–300 nm) will be overestimated and appear as particles of 250–300 nm regardless of their length. Single-molecule localization microscopy allows pushing the spatial resolution down to the nanometer scale, but it requires fixed samples and the temporal information provided by TIRFM is lost. Structured illumination microscopy (SIM) combined with TIRFM is then a good compromise to achieve a spatial resolution of ~100–150 nm and fast imaging acquisition (more than one frame per second). SIM-TIRFM allowed the anisotropic morphology of the diffraction-limited MreB filamentous assemblies to be revealed in *B. subtilis* [16].

Acknowledgment

References

1. Jones LJ, Carballido-López R, Errington J (2001) Control of cell shape in bacteria: helical, actin-like filaments in *Bacillus subtilis*. Cell 104(6):913–922

2. van den Ent F, Amos LA, Löwe J (2001) Prokaryotic origin of the actin cytoskeleton. Nature 413(6851):39–44

3. Billaudeau C, Chastanet A, Yao Z, Cornilleau C, Mirouze N, Fromion V, Carballido-Lopez R (2017) Contrasting mechanisms of growth in two model rod-shaped bacteria. Nat Commun 8:15370. https://doi.org/10.1038/ncomms15370

4. Dominguez-Escobar J, Chastanet A, Crevenna AH, Fromion V, Wedlich-Soldner R, Carballido-Lopez R (2011) Processive movement of MreB-associated cell wall biosynthetic complexes in bacteria. Science 333 (6039):225–228. https://doi.org/10.1126/science.1203466

5. Garner EC, Bernard R, Wang W, Zhuang X, Rudner DZ, Mitchison T (2011) Coupled, circumferential motions of the cell wall synthesis machinery and MreB filaments in B. subtilis. Science 333(6039):222–225

6. Axelrod D, Burghardt TP, Thompson NL (1984) Total internal reflection fluorescence. Annu Rev Biophys Bioeng 13:247–268. https://doi.org/10.1146/annurev.bb.13.060184.001335

7. Fish KN (2009) Total internal reflection fluorescence (TIRF) microscopy. Curr Protoc Cytom Chapter 12:Unit12.18. https://doi.org/10.1002/0471142956.cy1218s50

8. Jaqaman K, Loerke D, Mettlen M, Kuwata H, Grinstein S, Schmid SL, Danuser G (2008) Robust single-particle tracking in live-cell time-lapse sequences. Nat Methods 5 (8):695–702. https://doi.org/10.1038/nmeth.1237

9. Tinevez JY, Perry N, Schindelin J, Hoopes GM, Reynolds GD, Laplantine E, Bednarek SY, Shorte SL, Eliceiri KW (2017) TrackMate: an open and extensible platform for single-particle tracking. Methods 115:80–90. https://doi.org/10.1016/j.ymeth.2016.09.016

10. Schindelin J, Arganda-Carreras I, Frise E, Kaynig V, Longair M, Pietzsch T, Preibisch S, Rueden C, Saalfeld S, Schmid B, Tinevez JY, White DJ, Hartenstein V, Eliceiri K, Tomancak P, Cardona A (2012) Fiji: an open-source platform for biological-image analysis. Nat Methods 9(7):676–682. https://doi.org/10.1038/nmeth.2019

11. Applegate KT, Besson S, Matov A, Bagonis MH, Jaqaman K, Danuser G (2011) plusTip-Tracker: quantitative image analysis software for the measurement of microtubule dynamics. J Struct Biol 176(2):168–184. https://doi.org/10.1016/j.jsb.2011.07.009

12. Ducret A, Quardokus EM, Brun YV (2016) MicrobeJ, a tool for high throughput bacterial cell detection and quantitative analysis. Nat Microbiol 1(7):16077. https://doi.org/10.1038/nmicrobiol.2016.77

13. Paintdakhi A, Parry B, Campos M, Irnov I, Elf J, Surovtsev I, Jacobs-Wagner C (2016) Oufti: an integrated software package for high-accuracy, high-throughput quantitative microscopy analysis. Mol Microbiol 99 (4):767–777. https://doi.org/10.1111/mmi.13264

14. Stylianidou S, Brennan C, Nissen SB, Kuwada NJ, Wiggins PA (2016) SuperSegger: robust image segmentation, analysis and lineage tracking of bacterial cells. Mol Microbiol 102 (4):690–700. https://doi.org/10.1111/mmi.13486

15. Manley S, Gillette JM, Patterson GH, Shroff H, Hess HF, Betzig E, Lippincott-Schwartz J (2008) High-density mapping of single-molecule trajectories with photoactivated localization microscopy. Nat Methods 5 (2):155–157. https://doi.org/10.1038/nmeth.1176

16. Billaudeau C, Yao Z, Cornilleau C, Carballido-Lopez R, Chastanet A (2019) MreB forms sub-diffraction nanofilaments during active growth in Bacillus subtilis. MBio 10(1):e01879-18. https://doi.org/10.1128/mBio.01879-18